01 Jan 1990

Robust Nonlinear Control of Brushless DC Motors for Direct-Drive Robotic Applications

N. Hemati

J. S. Thorp

Ming-Chuan Leu
Missouri University of Science and Technology, mleu@mst.edu

Recommended Citation

N. Hemati et al., "Robust Nonlinear Control of Brushless DC Motors for Direct-Drive Robotic Applications," *IEEE Transactions on Industrial Electronics*, Institute of Electrical and Electronics Engineers (IEEE), Jan 1990.
The definitive version is available at https://doi.org/10.1109/41.103449

Robust Nonlinear Control of Brushless dc Motors for Direct-Drive Robotic Applications

NEYRAM HEMATI, MEMBER, IEEE, JAMES S. THORP, FELLOW, IEEE AND MING C. LEU, MEMBER, IEEE

***Abstract*—The control problem associated with brushless dc motors (BLDCM) for direct-drive robotic applications is considered. In order to guarantee the high-performance operation of BLDCM's in such applications, the effects of reluctance variations and magnetic saturation are accounted for in the model. Such a BLDCM model constitutes a highly coupled and nonlinear dynamic system. Using the transformation theory of nonlinear systems, a feedback control law, which is shown to compensate for the system nonlinearities, is derived. Conditions under which such a control law is possible are presented. Furthermore, the need for the derivation of explicit commutation strategies is eliminated, resulting in the reduction of the computations involved. To guarantee the high-performance operation of the system subject to substantial uncertainties, a robust control law is derived and appended to the overall control structure. The inclusion of the robust controller results in good tracking performance when there are modeling and measurement errors and payload uncertainties. The efficacy of the overall control law is investigated by considering a single-link direct-drive arm actuated by a BLDCM.**

I. Introduction

ROBUST tracking control of brushless dc motors (BLDCM) for direct-drive robotic applications is considered. This study has been motivated by the increasing potential and interest in adopting BLDCM for high-performance applications such as direct-drive robotics [1], [5], [14]. Until recently, the use of brushless motors had been limited due to the high cost of the electronic circuitry associated with them. However, due to the recent advancements in power electronics, brushless motors are replacing their brushed counterparts and are becoming the dominant actuators for high-performance applications. Furthermore, due to the continuing breakthroughs and reduction of costs in power electronics, the real-time implementation of advanced control schemes is becoming feasible [9], [10], thus resulting in the possibility of achieving better performance in the future.

BLDCM's have been an attractive choice for direct-drive robotics [1], mainly because of their large torque-producing capabilities, which are suitable for high acceleration and deceleration rates. In a direct-drive servo system, the load is directly coupled to the motor, and therefore, the torque generated by the motor is directly transmitted to the load. As a result, in order to ensure high performance of the system, the full dynamics of the motor and its interaction with the load must be taken into account. To guarantee the high-performance operation of BLDCM's in such motion control applications, the effects of magnetic saturation and reluctance variations must be taken into account. Another class of motors, which has been regarded as being attractive for direct-drive applications, is the variable reluctance motor (VRM) [1], [9]. In VRM's, the mutual couplings among the phase windings are negligible [9], [10], whereas in a BLDCM, the mutual inductances play a significant role [5]. This introduces a major difficulty in terms of constructing the mathematical model and deriving commutation strategies for control purposes when magnetic saturation is present [5], [7]. The proposed approach, in this paper, eliminates the need for the derivation of explicit commutation strategies.

The BLDCM's under study constitute multivariable, coupled, nonlinear systems. Therefore, the tracking control problem associated with them is addressed in the context of tracking control of multivariable nonlinear systems. As the first step in the control design process, a feedback linearizing control law is derived, which compensates for the system nonlinearities. It is demonstrated that this control law, in conjunction with linear state feedback control, provides good dynamic performance in the presence of uncertainties. However, the performance of this control law is shown to be degraded if accurate feedback measurements are unavailable. To alleviate this problem, and to guarantee good performance of the system in the presence of bounded uncertainties in the model and the measurements [3], [4], [11], [13], a robust control term is derived and appended to the feedback linearizing controller. Computer simulations are used to examine the effectiveness of the proposed control when the BLDCM direct-drive system is subject to modeling, payload, and measurement uncertainties.

The paper is organized as follows. In Section II, we describe the system that will be studied throughout the paper. The mathematical model associated with BLDCM with magnetic saturation and reluctance variations is presented and discussed in some detail. In addition, experimental data are provided to demonstrate the validity of the BLDCM model that is used. In Section III, the feedback linearizing control law is derived, which demonstrates good tracking perfor-

Manuscript received September 25, 1989; revised July 7, 1990. This work was supported by Moog Inc., East Aurora, NY, and by NSF Grant MSM8451074.

N. Hemati is with the Department of Mechanical Engineering and Mechanics, Drexel University, Philadelphia, PA 19104.

J. S. Thorp is with the Department of Electrical Engineering, Cornell University, Ithaca, NY 14853.

M. C. Leu is with the Department of Mechanical and Industrial Engineering, New Jersey Institute of Technology, Newark, NJ 07102.

IEEE Log Number 9040012.

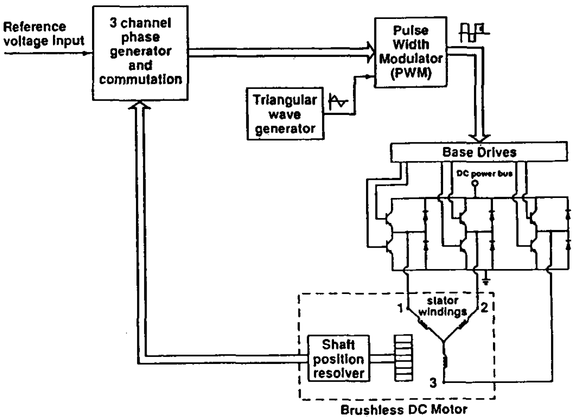

Fig. 1. Typical configuration for a BLDCM and its commutation.

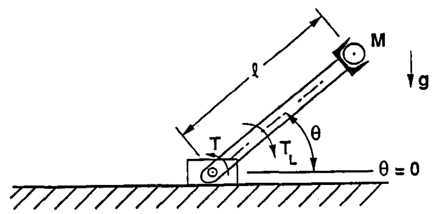

Fig. 2. Direct-drive arm actuated by a BLDCM. $l = 1.0$ m, $M = 2.0$ kg. The link is assumed massless.

mance in the absence of measurement uncertainties. The robust controller is presented in Section IV. In Section V, simulation results are presented for a direct-drive system composed of a BLDCM and a one-degree-of-freedom robot arm.

II. Mathematical Model of BLDCM and the Direct-Drive Arm

A BLDCM consists of a permanent magnet rotor, a position sensor mounted on the rotor, and a means to provide signals to the stator windings (see Fig. 1). The signals to the phase windings are synchronized with the output from the position sensor to provide the electronic commutation. The armature windings (located on the stator) of a typical BLDCM are three-phase, Y-connected, and sinusoidally distributed [1], [11]. Here, a one-degree-of-freedom inverted pendulum (robot arm) actuated by a BLDCM is considered (see Fig. 2). The motor will generate a prescribed torque profile such that the payload and the arm are guided along a given trajectory that is specified in terms of the time histories of position, velocity, and acceleration. For the payload to track the prescribed trajectory, appropriate control commands (voltages/currents) must be supplied to the motor windings. In turn, it is the performance of the motor that determines how accurately the trajectory is tracked. In this section, a BLDCM model which accounts for magnetic saturation and reluctance variations, is presented. Some experimental data are presented to demonstrate the validity of the proposed model.

A. BLDCM with Linear Magnetic Structure

In the absence of magnetic saturation, it is convenient to formulate the dynamic behavior of a BLDCM in the d-q-0 coordinate frame as follows [2], [5], [11]:

$$v_q = Ri_q + n\lambda_d \frac{d\theta}{dt} + \frac{d\lambda_q}{dt} \tag{1a}$$

$$v_d = Ri_d - n\lambda_q \frac{d\theta}{dt} + \frac{d\lambda_d}{dt} \tag{1b}$$

where R is phase resistance, v is voltage, i is current, θ is angular displacement, n is number of pole pairs, λ is flux linkage, and t represents time. The torque function may be written as

$$T(i_q, i_d) = \left(\frac{3n}{2}\right)(\lambda_d i_q - \lambda_q i_d). \tag{2}$$

The flux linkages may be written in terms of the constant inductance parameters L_q and L_d and the electromotive force constant K_e as follows:

$$\lambda_q = L_q i_q \tag{3}$$

$$\lambda_d = L_d i_d + K_e. \tag{4}$$

L_q and L_d represent fictitious inductance quantities that are related to the stator phase winding inductances in the following way[1]:

$$L_q = \left(\frac{3}{2}\right)(L_a - L_g) \tag{5a}$$

$$L_d = \left(\frac{3}{2}\right)(L_a + L_g) \tag{5b}$$

where L_a is the average inductance of the phase windings, and L_g represents the amplitude of the sinusoidal variations in the phase winding inductances due to the rotor displacement. In other words, L_g represents the degree of reluctance variations in the air gap.

To complete the mathematical model, the motion of the rotor and the arm are described by

$$\frac{d\theta}{dt} = \omega \tag{6a}$$

$$J_m \frac{d\omega}{dt} = T(i_q, i_d) - T_l(t) \tag{6b}$$

$$Ml^2 \frac{d^2\theta}{dt^2} + Mgl\cos(\theta) = T_l(t) \tag{6c}$$

where ω is angular velocity, J_m is the motor inertia, M is the payload mass, l is the distance from the joint axis to the payload, and $T_l(t)$ represents the load torque. Equations (6b) and (6c) may be combined to obtain

$$J\frac{d\omega}{dt} = T(i_q, i_d) - T_L(t) \tag{6d}$$

[1] The phase inductances and the electromotive force constant, as used in the formulation of the mathematical model, correspond to the line-to-neutral quantities.

where $J = J_m + Ml^2$ is the effective inertia, and T_L is the effective load torque.

B. BLDCM with Magnetic Saturation

The validity of the BLDCM model presented above is solely based on the assumption that the magnetic structure of the motor retains its linearity throughout the operation. In other words, the BLDCM mathematical model presented above is valid if the inductance parameters L_a and L_g and the electromotive force constant K_e remain constant. In the presence of magnetic saturation, however, these parameters can no longer be assumed to be constants throughout the operation. To include the effect of magnetic saturation in the mathematical model, the variations of these parameters must be formulated as functions of phase currents. In [5], it was shown that these variations could be modeled by a set of piecewise continuous polynomials as follows:

$$K_e(i) = \frac{\alpha_0 + \alpha_1 i + \alpha_2 i^2 + \alpha_3 i^3}{n\sqrt{3}\, i} \tag{7a}$$

$$L_g(i) = \frac{\beta_0 + \beta_1 i + \beta_2 i^2 + \beta_3 i^3 + \beta_4 i^4}{3ni^2} \tag{7b}$$

$$L_a(i) = KL_g(i) \tag{7c}$$

where

$$i = \sqrt{\frac{i_q^2 + i_d^2}{2}} \tag{8}$$

and where α_j $(j = 1, \cdots)$, β_k $(k = 1, \cdots)$ and K are constant coefficients. Based on an experimental procedure, through which a set of four-dimensional surfaces corresponding to the phase flux linkages and the electromagnetic torque function are identified, the numerical values for the coefficients in (7a)–(7c) can be computed [5].

To be able to take advantage of the simple structure associated with the BLDCM model in the d-q-0 coordinate frame, the inductance parameters and the electromotive force constant are modeled to be piecewise constant functions of the phase current variable i. In other words, these parameters are considered constant in prescribed intervals of current. It is important to note that since the variations in L_a, L_g, and K_e have been accurately characterized, by (7a)–(7c), the width of the current intervals may be chosen to be arbitrarily small. To establish the validity of the proposed modeling procedure, Figs. 3 and 4 illustrate the comparisons between the experimental results and the corresponding predicted values obtained from the mathematical model. As is evident from the figures, the agreement is quite reasonable. Furthermore, the results indicate the significance of reluctance variations (Fig. 3) and the degree of magnetic saturation that is present (Fig. 4).

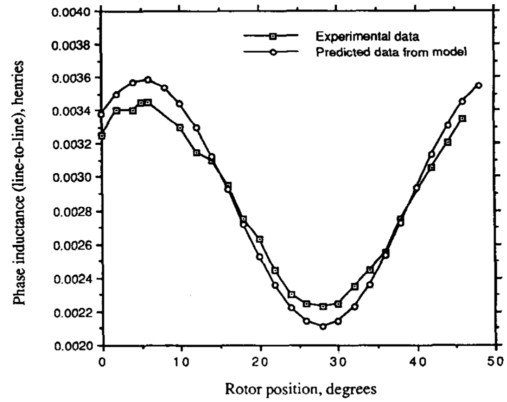

Fig. 3. Experimental and predicted values of phase winding inductance in the linear magnetic range.

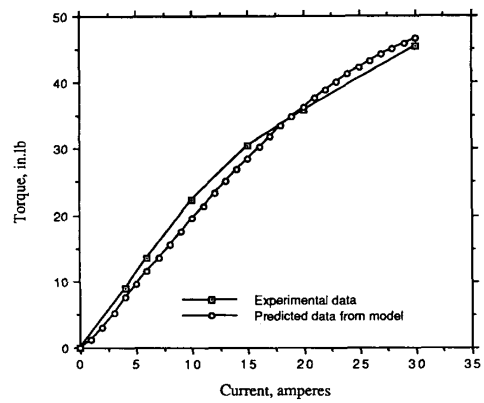

Fig. 4. Experimental and predicted plots of torque-current characteristics at rotor speed of 200 r/min.

III. Nonlinear Control of BLDCM and the Direct-Drive Arm

In the past, the control problem associated with BLDCM's has mostly been addressed based on simplified linear models, e.g., [1]. Namely, the following assumptions have been made: 1) The reluctance variations are insignificant, i.e., $L_g = 0$; 2) the d-axis dynamics may be neglected; 3) the saturation effects may be neglected. As a result of these assumptions, a BLDCM model resembling that of a conventional dc motor is obtained, making the control problem similar to that associated with a conventional dc motor. Here, these assumptions are relaxed, and the full dynamics of a BLDCM are included in the derivation of the control law.

The tracking control problem associated with BLDCM's is attacked as a feedback linearizing control problem [8]. A nonlinear dynamic system

$$\frac{dx}{dt} = f(x) + G(x)u(t) \tag{9}$$

where $f(x)$: $R^n \rightarrow R^n$ and $G(x)$: $R^n \rightarrow R^{n \times m}$ are smooth vector fields, is said to be feedack linearizable if there exist 1) a neighborhood U in R^n of the origin, 2) a differentiable transformation with a differentiable inverse $T(x)$: $R^n \rightarrow R^n$, and 3) the nonlinear feedback

$$\nu(t) = \beta(x)u(t) + \sigma(x) \tag{10}$$

with $\beta(x)$: $R^n \rightarrow R^{m \times m}$ being nonsingular, such that the transformed state vector

$$z(t) = T(x) \tag{11}$$

satisfies the linear system of differential equations

$$\frac{dz}{dt} = Az(t) + B\nu(t) \tag{12}$$

where the pair (A, B) is in the appropriate Brunovsky canonical form with the Kronecker indices $\kappa_1, \kappa_2, \ldots, \kappa_m$.

The necessary and sufficient conditions [8] for the nonlinear system (9) to be feedback linearizable are that for a neighborhood U in R^n, the following must be satisfied: 1) The vector fields $\{G_1, [f, G_1], \cdots, (ad^{\kappa_1 - 1}f, G_1), \cdots, G_m, [f, G_m], \cdots, (ad^{\kappa_m - 1}f, G_m)\}$[2] are linearly independent; 2) the sets $C_j = \{G_1, \cdots, (ad^{\kappa_j - 2}f, G_1), \cdots, G_m, \cdots, (ad^{\kappa_j - 2}f, G_m)\}$ for $j = 1, 2, \cdots, m$ are involutive[3]; 3) the sets C_j span the same space as $C_j \cap C$. In the following section, conditions are derived defining the regions in which the BLDCM model is feedback linearizable.

A. Transformation to the Linear System

In this section, we address the feedback linearizing control of a BLDCM. The need to derive explicit commutation strategies as in [9] and [10] is eliminated because we have described the BLDCM dynamics in the *d-q-*0 coordinate frame, where the flux linkages and the torque function are represented as functions that are independent of the rotor position. For convenience, we will rearrange and write the BLDCM governing the equations in the following form:

$$\frac{d\theta}{dt} = \omega \tag{13a}$$

$$\frac{d\omega}{dt} = \frac{1}{J}\left\{\frac{3n}{2}\left[K_e i_q + (L_d - L_q) i_d i_q\right] - T_L(t)\right\} \tag{13b}$$

$$\frac{di_q}{dt} = \frac{1}{L_q}\left\{v_q - Ri_q - nL_d i_d \frac{d\theta}{dt} - nK_e \frac{d\theta}{dt}\right\} \tag{13c}$$

$$\frac{di_d}{dt} = \frac{1}{L_d}\left\{v_d - Ri_d + nL_q i_q \frac{d\theta}{dt}\right\}. \tag{13d}$$

To keep the formulation in a generalized framework, no specific form of $T_L(t)$ will be assumed, with the exception that $T_L(t)$ is assumed to be a smooth function of time. Comparing the BLDCM governing equations, i.e., (13a)–(13d), to the system defined by (9), one can define the following

$$f(x) = \begin{bmatrix} x_2 \\ x_3 \\ k_1 x_4 + k_2 x_4 x_5 - T_L \\ -k_4 x_3 - k_3 x_4 - k_5 x_3 x_5 \\ -k_6 x_5 + k_7 x_3 x_4 \end{bmatrix} \tag{14a}$$

$$G(x) = \begin{bmatrix} 0 & 0 & 0 & q_1 & 0 \\ 0 & 0 & 0 & 0 & q_2 \end{bmatrix}^T \tag{14b}$$

$$x(t) = \left[\int \theta\, dt \quad \theta \quad \omega \quad i_q \quad i_d\right]^T \tag{14c}$$

$$u(t) = \begin{bmatrix} v_q \\ v_d \end{bmatrix} \tag{14d}$$

where $k_1 = 3nK_e/2J$, $k_2 = 3n(L_d - L_q)/2J$, $k_3 = R/L_q$, $k_4 = nK_e/L_q$, $k_5 = nL_d/L_q$, $k_6 = R/L_d$, $k_7 = nL_q/L_d$, $q_1 = 1/L_q$, $q_2 = 1/L_d$. Note that the integral of position has been added as a new state for the convenience of including an integral control term in the pole-placement controller of Section III-C.

We will now apply the necessary and sufficient conditions given in Section III-A to the BLDCM system, i.e., (14a)–(14d). Note that if it is possible to obtain a control law to transform the governing equations to a linear system equivalent, then to achieve the desired dynamic performance, one is left with a linear control problem. It will be shown below that the necessary and sufficient conditions for the existence of $T(x)$ are satisfied for $\kappa_1 = 4$, $\kappa_2 = 1$. First, the set $C = \{G_1, [f, G_1], (ad^2 f, G_1), (ad^3 f, G_1), G_2\}$ spans a five-dimensional space. To show this, we will construct the matrix whose columns are the vectors in the set C, as follows:

$$\begin{bmatrix} 0 & 0 & 0 & -q_1(k_1 + k_2 x_5) & 0 \\ 0 & 0 & q_1(k_1 + k_2 x_5) & C_{24} & 0 \\ 0 & -q_1(k_1 + k_2 x_5) & C_{33} & C_{34} & 0 \\ q_1 & q_1 k_3 & C_{43} & C_{44} & 0 \\ 0 & -q_1 k_7 x_3 & C_{53} & C_{54} & q_2 \end{bmatrix}. \tag{15}$$

Obviously, this matrix has full rank, as long as the following condition is satisfied:

$$k_1 + k_2 x_5 \neq 0. \tag{16}$$

Second, the set $C_1 = \{G_1, [f, G_1], (ad^2 f, G_1), G_2, [f, G_2]\}$ and the set C_2 are involutive. C_2 is trivially involutive since it is empty. To show the involutivity of C_1, it can be demonstrated that Lie brackets $[G_1, [f, G_1]]$, $[G_1, (ad^2 f, G_1)]$, $[G_1, G_2]$, $[G_1, [f, G_2]]$, $[[f, G_1], (ad^2 f, G_1)]$, $[[f, G_1], G_2]$, $[[f, G_1], [f, G_2]]$, $[(ad^2 f, G_1), G_2]$, $[(ad^2 f,$

---

[2] $[f, G_j]$, $(ad^2 f, G_j), \cdots,$ and $(ad^k f, G_j)$ denote the Lie brackets of the vector fields f and G_j and are defined as follows:

$$[f, G_j] = (ad^1 f, G_j) = \frac{\partial G_j}{\partial x} f - \frac{\partial f}{\partial x} G_j$$

$$\text{and } (ad^k f, G_j) = [f, (ad^{k-1} f, G_j)].$$

[3] A set S composed of vector fields in R^n is said to be involutive if the Lie bracket of any pair of vector fields in S can be expressed as a linear combination of the vector fields in S, where the coefficients in the linear combination are allowed to be smooth functions in R^n.

G_1, $[f, G_2]]$, $[G_2, [f, G_2]]$ can be written as a linear combination of the elements of C_1. Finally, the span of C_1 (C_2) is clearly equal to the span of the intersection of C_1 (C_2) and C.

Having demonstrated the existence of a transformation, i.e., change of coordinates $z(t) = T(x)$, which transforms the BLDCM nonlinear system description to a controllable linear system in the Brunovsky canonical form with the Kronecker indices $\kappa_1 = 4$, $\kappa_2 = 1$, we may now attempt to derive a control law of the form (10), which will result in the transformation of the BLDCM description ((14a)–(14d)) to a linear system description of the form given by (12), where

$$z(t) = \begin{bmatrix} \int \theta \, dt \\ \theta \\ \omega \\ \alpha \\ i_d \end{bmatrix}; \quad A = \begin{bmatrix} 0 & 1 & 0 & 0 & 0 \\ 0 & 0 & 1 & 0 & 0 \\ 0 & 0 & 0 & 1 & 0 \\ 0 & 0 & 0 & 0 & 0 \\ 0 & 0 & 0 & 0 & 0 \end{bmatrix};$$

$$B = \begin{bmatrix} 0 & 0 \\ 0 & 0 \\ 0 & 0 \\ 1 & 0 \\ 0 & 1 \end{bmatrix}. \tag{17}$$

B. Derivation of the Feedback Linearizing Controller

To proceed with the derivation of the feedback linearizing control law, it is helpful to consider the following. The control commands v_q and v_d will be designed to achieve the following objectives: 1) compensate for the nonlinearities and decouple the dynamics; 2) guide the payload along a given trajectory; 3) provide robustness. The third objective will be addressed in Section IV. The first objective is identical to deriving the feedback linearizing controller. To achieve this, the control voltages are derived such that the system equations (13a)–(13d) are transformed to the following linear controllable form

$$\frac{d\theta}{dt} = \omega \tag{18a}$$

$$\frac{d\omega}{dt} = \alpha \tag{18b}$$

$$\frac{d\alpha}{dt} = v_1 \tag{18c}$$

$$\frac{di_d}{dt} = v_2 \tag{18d}$$

where v_1 and v_2 are the control commands of the transformed linear system, and α is acceleration. To derive the v_q and v_d, which will accomplish this transformation, we will proceed as follows:

$$\frac{d\alpha}{dt} = \frac{1}{J}\left\{\frac{dT(i_q, i_d)}{dt} - \frac{dT_L}{dt}\right\} \tag{19}$$

which can be written as

$$\frac{d\alpha}{dt} = \frac{1}{J}\left\{\frac{\partial T(i_q, i_d)}{\partial i_q}\frac{di_q}{dt} + \frac{\partial T(i_q, i_d)}{\partial i_d}\frac{di_d}{dt} - \frac{dT_L}{dt}\right\} \tag{20}$$

Recalling (2)–(4), we then get

$$\frac{\partial T(i_q, i_d)}{\partial i_q} = \left(\frac{3n}{2}\right)\{K_e + (L_d - L_q)i_d\} \tag{21}$$

$$\frac{\partial T(i_q, i_d)}{\partial i_d} = \left(\frac{3n}{2}\right)(L_d - L_q)i_q. \tag{22}$$

By substituting (21) and (22) in (20) and proceeding further, the following is arrived at:

$$\begin{aligned} v_q = &\left\{\left(\frac{2L_q}{3n}\right)\left(Jv_1 + \frac{dT_L}{dt}\right) - \left(\frac{L_q}{L_d}\right)\right. \\ &\left.\cdot\{(L_d - L_q)i_q\}\{v_d - Ri_d + nL_q i_q \omega\}\right\} \\ &\cdot\{K_e + (L_d - L_q)i_d\}^{-1} \\ &+ Ri_q + n\omega(L_d i_d + K_e). \end{aligned} \tag{23}$$

In a similar manner and by comparing (18d) and (13d), one will get

$$v_d = L_d v_2 + Ri_d - nL_q i_q \omega. \tag{24}$$

As is evident from (23), the control voltage v_q is computable if

$$K_e + (L_d - L_q)i_d \neq 0. \tag{25}$$

This condition is likely to always hold since, in general, magnitude of K_e is much larger than $|L_d - L_q|$[4], suggesting that condition (25) is violated only for very large values of i_d.[5] Moreover, as described in the following paragraph, the d-axis controller is designed to stabilize i_d at zero, providing further assurance for the existence of the feedback linearizing controller.

To accomplish the second objective, i.e., to guide the payload along a prescribed trajectory, a tracking controller in terms of the transformed control inputs v_1 and v_2 is designed. Observing that the control input v_2 affects the dynamics of the d-axis current variable, to eliminate the effect of the d-axis current on the generated torque, v_2 is designed to drive i_d to zero as fast as possible. Consequently, the control input v_1 will be given the full authority to achieve zero tracking error.

[4] The BLDCM's under study have the following specifications in the linear magnetic range:

$$K_e = 0.02502 \text{ V/rad/s}, \; L_a = 0.95 \text{ mH}, \; L_g = 0.2 \text{ mH}, \; R = 0.9\,\Omega$$

where the values are based on line-to-neutral measurements.

[5] For example, if one uses the nominal values for the parameters of the BLDCM under study, (25) will be violated for $i_d = 417$ A.

C. Pole-Placement Control

The feedback linearizing control, which is expressed in (23) and (24), can be written as

$$\nu(t) = \begin{bmatrix} v_1 \\ v_2 \end{bmatrix} = \beta(x)u(t) + \sigma(x) \tag{26}$$

where

$$\beta(x) = \begin{bmatrix} (k_1 + k_2 x_5)q_1 & q_2 k_2 x_4 \\ 0 & q_2 \end{bmatrix} \tag{27}$$

$$\sigma(x) = \begin{bmatrix} -(k_1 + k_2 x_5)(k_3 x_4 + k_4 x_3 + k_5 x_3 x_4) - k_2 x_4 (k_6 x_5 - k_7 x_3 x_4) + \dfrac{1}{J}\dfrac{dT_L}{dt} \\ -k_6 x_5 + k_7 x_3 x_4 \end{bmatrix}. \tag{28}$$

The control law defined by (23) and (24) transforms the nonlinear system of (13a)–(13d) to the linear canonical form (18a)–(18d). Since at this point one is left with a linear system, the controls v_1 and v_2 can be designed based on linear control system techniques. Since we are interested in tracking a desired trajectory, it is convenient to replace the state vector $z(t)$ of (12) and (17) with a new state vector $y(t)$ as follows:

$$y(t) = \left[\int (\theta_d - \theta)\, dt \quad \theta_d - \theta \quad \omega_d - \omega \quad \alpha_d - \alpha \quad i_d \right]^T \tag{29}$$

where θ_d, ω_d, and α_d are the time histories of position, velocity, and acceleration, respectively, of the desired trajectory.

Assuming that the system nonlinearities have been compensated for, in order to achieve the desirable dynamic response for the overall system, we will use a pole-placement controller in conjunction with the linearized system. The following state feedback law is considered

$$\nu(t) = Hy(t) \tag{30}$$

where

$$H = \begin{bmatrix} h_1 & h_2 & h_3 & h_4 & 0 \\ 0 & 0 & 0 & 0 & h_5 \end{bmatrix}. \tag{31}$$

The elements of H are appropriately chosen based on a desirable reference model. We specify the characteristic equation of the reference model as

$$F(\lambda) = (\lambda + h_5)(\lambda^2 + 2\xi\omega_1 + \omega_1^2)(\lambda^2 + 2\xi\omega_2 + \omega_2^2). \tag{32}$$

Once the feedback control law for the linear system has been specified, the nonlinear control can be computed by

$$u(t) = \beta^{-1}(x)\{Hy(t) - \sigma(x)\}. \tag{33}$$

Clearly, in order for the feedback linearizing controller to exist, the matrix $\beta(x)$ must be invertible. The invertibility of $\beta(x)$ is guaranteed if (16), or equivalently (25), is satisfied. As will be shown in the simulation results of Section V, the proposed control law of this section behaves well even if the system is subject to significant payload uncertainties and modeling errors, provided that accurate measurements of acceleration are available. If, however, estimated acceleration information is to be used, which is the case is most practical situations, the performance of the system may be drastically degraded. To account for modeling, payload, and measurement errors, a robust control law will be presented in the following section.

IV. Robust Control

In this section, a nonlinear robust controller is designed and appended to the control law of the previous section. The controller is robust in the sense that in the presence of bounded uncertainties in the model, the tracking error envelope is bounded. Furthermore, as will be shown below, the size of the tracking error envelope can be altered through the proper choice of control parameters. The overall controller shall be used for position tracking control of the direct-drive arm actuated by a BLDCM. The overall control is specified to be

$$u(t) = u_n(t) + \Delta u(t) \tag{34}$$

where $u_n(t)$ corresponds to the control law of Section III, and $\Delta u(t)$ represents the correction term that will make the system robust. In the absence of uncertainties, the control $u_n(t)$ will provide good dynamic response. $\Delta u(t)$, which is a saturating function, will guarantee robustness in the presence of uncertainties.

Assuming that there are uncertainties in the mathematical model of the system, to distinguish between the actual system and the system model in our previous derivations, the system model is represented by $f^*(x)$ and $G^*(x)$, and the following are defined

$$\Delta f = f - f^* \tag{35a}$$

$$\Delta G = G - G^*. \tag{35b}$$

The derivation of the robust controller for the BLDCM system will be proceeded following the framework provided in [3], [4], and [12]. One of the basic assumptions needed is what are usually known as the matching conditions, which implies that the dynamics of the system are affected by the control input in the same manner that the uncertainties are affected. To enforce this assumption, we introduce Δf^* and ΔG^*, which satisfy the following conditions

$$\frac{\partial T}{\partial x}\Delta f = B\Delta f^* = B\begin{bmatrix} \Delta f_1^* \\ \Delta f_2^* \end{bmatrix} \tag{36a}$$

$$\frac{\partial T}{\partial x}\Delta G = B\Delta G^*\beta = B\begin{bmatrix} \Delta G_1^* & \Delta G_2^* \\ \Delta G_3^* & \Delta G_4^* \end{bmatrix}\beta. \tag{36b}$$

Through the application of the transformation $T(x)$, conditions (36a) and (36b) become

$$(A - A^*)T(x) = \Delta A\ T(x) = B[\Delta f^* - \Delta G^*\sigma] \quad (37a)$$

$$B - B^* = \Delta B = B\Delta G^*. \quad (37b)$$

By imposing the matching conditions (37a)–(37b), two things have been achieved. First, the system uncertainties have now been imbedded in Δf^* and ΔG^*, and second, it is shown that the uncertainties are affected in the same way as the input to the system is affected by matrix B. Applying conditions (37a) and (37b) to the system under consideration, we get

$$\frac{d\Delta y}{dt} = B(\Delta G^* \beta u_n + \Delta f^*). \quad (38)$$

Having assumed bounded uncertainties, we can define ϕ such that

$$\phi \geq \|\Delta G^* \beta u_n + \Delta f^*\| \quad (39)$$

to provide a measure for the bound on uncertainties. Assuming that accurate measurements for y_1, y_2, and y_3 in (29) are available (a realistic assumption), we can obtain Δf^* and ΔG^* as follows:

$$\Delta f_1^* = -(k_1 + k_2 x_5)\Delta f_4 - k_2 x_4 \Delta f_5 \quad (40a)$$

$$\Delta f_2^* = \Delta f_5 \quad (40b)$$

$$\Delta G_1^* = -\delta q_1 \quad (40c)$$

$$\Delta G_2^* = k_2 x_4(\delta q_1 - \delta q_2) \quad (40d)$$

$$\Delta G_3^* = 0 \quad (40e)$$

$$\Delta G_4^* = \delta q_2 \quad (40f)$$

where $\delta q_1 = \Delta q_1 / q_1$ and $\delta q_2 = \Delta q_2 / q_2$.

At this point, we have developed a set of explicit formulae for the bounds imposed on the modeling errors of our system, which can be estimated in quantitative terms. For example, δq_1 and δq_2 express bounds for the percentage errors in inductance values. The correction term Δu in the control law, which should provide robustness, is defined in terms of the uncertainty bound ϕ and a saturating function as follows:

$$\Delta u = -\phi \beta^{-1} \eta(\zeta) \quad (41)$$

where

$$\eta(\zeta) = \begin{cases} \zeta & \text{if } \|\zeta\| \leq 1 \\ \zeta / \|\zeta\| & \text{if } \|\zeta\| \geq 1 \end{cases} \quad (42)$$

Furthermore

$$\zeta = \pi \phi B^T P^{-T} P^{-1} y \quad (43)$$

where P is the matrix whose columns are the eigenvectors of the matrix $(A + BH)$, and π is a parameter that can be chosen to alter the bound on the tracking error. As will be shown in Section V, the controller presented above will provide bounded tracking errors in the presence of uncertainties.

V. Simulation Results

In this section, the proposed control schemes of Sections III and IV are used to control a one-degree-of-freedom robot arm that is actuated by the BLDCM whose model was presented in Section II-B. The full dynamics of a BLDCM, including magnetic saturation and reluctance variation effects, are accounted for. The task, defined in terms of a cubic position trajectory (Fig. 5), is designed such that the BLDCM operates well into the magnetic saturation region. The payload is to travel along this trajectory, moving from the horizontal plane, i.e., $\theta = 0$, to the vertical and upright position, i.e., $\theta = \pi/2$ radians, in 1 s. The linear controller gains, i.e. $h_1, \cdots, h_5$ in (31), are chosen such that the reference model (32) has two pairs of poles with natural frequencies $\omega_1 = \omega_2 = 6.4$ Hz and damping ratios $\zeta_1 = \zeta_2 = 1$. The controller gain h_5 corresponding to the current stabilizing control is set at 10^3. For the first set of simulation tests, we will start with the assumption that accurate measurements of states, including acceleration measurements, are available. However, it is expected that there will exist payload and modeling uncertainties, which the controller has to overcome. For example, Fig. 6 shows the time history of position error when the payload is to travel along the reference trajectory, and when payload inertia has been either underestimated or overestimated.

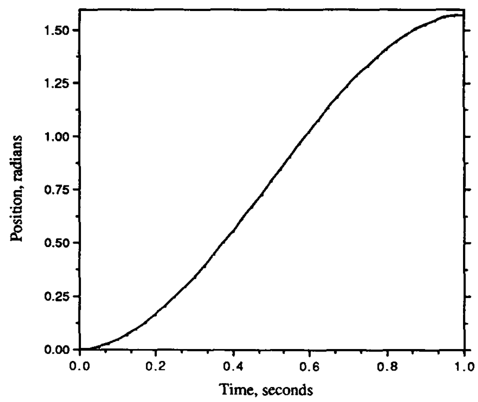

Fig. 5. Desired cubic position trajectory to be traversed by the payload.

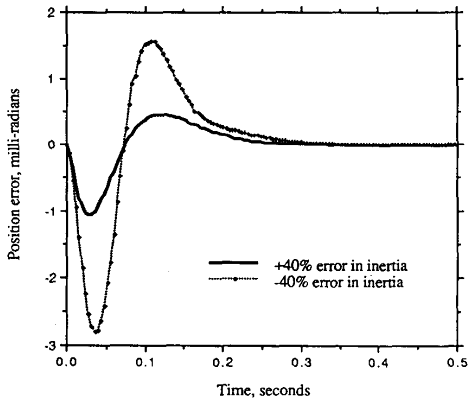

Fig. 6. Time histories of position error along the cubic trajectory using accurate acceleration measurements in the presence of payload uncertainties.

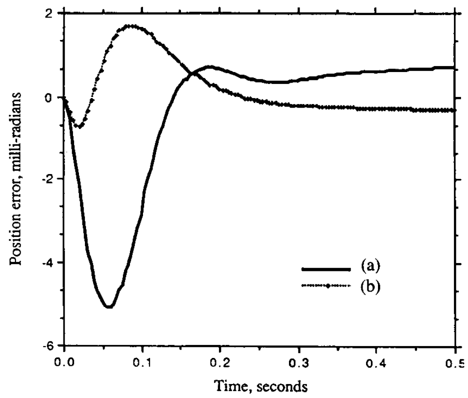

Fig. 7. Time histories of position error along the cubic trajectory using estimated acceleration measurements: (a) −40% error in inertia an +30% error in motor resistance; (b) +40% error in inertia and −30% error in motor resistance.

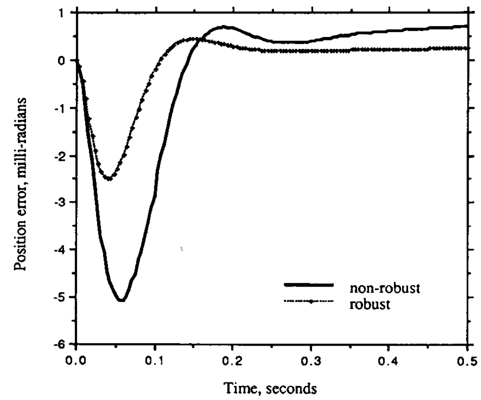

Fig. 8. Time histories of position error for the robust and nonrobust controllers using estimated acceleration measurements, −40% error in payload inertia, and +30% error in motor resistance. The robust control parameters are: $\pi = 10^{10}$, $\delta q_1 = \delta q_2 = 0.35$, $\Delta f_4 = \Delta f_5 = 10^{-5}$.

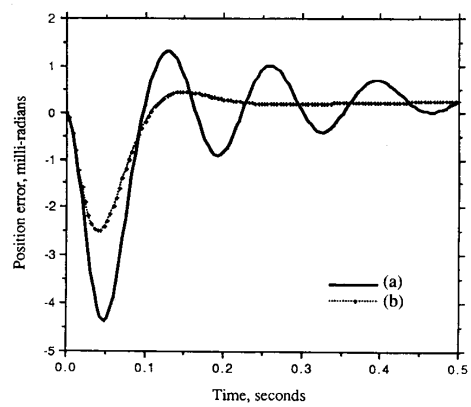

Fig. 9. Time histories of position error for the robust controller using estimated acceleration measurements, −40% error in payload inertia, and +30% error in motor resistance: (a) $\pi = 1$, $\delta q_1 = \delta q_2 = 0.35$, $\Delta f_4 = \Delta f_5 = 10^{-5}$; (b) $\pi = 10^{10}$, $\delta q_1 = \delta q_2 = 0.35$, $\Delta f_4 = \Delta f_5 = 10^{-5}$.

In a typical BLDCM system, direct acceleration measurements are seldom available. Consequently, for practical purposes, one must either eliminate the need for such measurements or use estimated feedback information [5]. The need for acceleration measurements may be eliminated if the control commands are supplied from a current source rather than a voltage source [5]. Alternatively, there are different schemes with which the acceleration information can be estimated. One way is to use the computed derivative of the velocity feedback in conjunction with the appropriate filtering techniques to eliminate the high-frequency noise. Another method, the method adopted here, is to predict the acceleration information based on the reference model in hand, i.e., use (13a)–(13d) and the modeled parameter values to estimate acceleration. Fig. 7 illustrates the performance of the system subject to uncertainties in the payload and the motor model when the acceleration information has been estimated based on the approximate system model. Obviously, the performance of the control law has deteriorated since inaccurate acceleration measurements have been used.

To alleviate the problem associated with inexact acceleration measurements, the robust control term, which was derived in Section IV, is appended to the nominal control law used in the simulations above. Fig. 8 depicts the performance of the robust controller when $\Delta f_4 = \Delta f_5 = 10^{-5}$, $\delta q_1 = \delta q_2 = 0.35$, and $\pi = 10^{10}$. It is evident from the figure that the tracking error profile has been improved, and the error envelope has been significantly reduced. It is interesting to study the effects of different control parameters on the performance of the controller. We will first look at the effect of π. Fig. 9 shows the tracking error for two different values of π, whereas other parameters remain the same as those used in Fig. 8. As expected, by increasing the value of π, the error envelope is made smaller. It is also important to study the effect of the size of the error bound imposed on the system, i.e., size of ϕ. For example, Fig. 10 shows the time histories of position error along the reference trajectory when δq_1 and δq_2 have been enlarged from 0.35 to 0.75. It is apparent from the figure that by imposing excessive error bounds, although we are able to reduce the size of the tracking error envelope, the error function contains undesirable oscillations.

VI. Conclusions

We have studied a direct-drive robotic arm system directly coupled to a BLDCM, which is capable of producing large torques for high acceleration and deceleration rates. The complete dynamics of the motor and the arm have been combined in investigating the tracking control problem associated with the system. To guarantee the high-performance operation of the system, the effects of magnetic saturation and reluctance variations have been accounted for in the BLDCM mathematical model. Some experimental data were presented to demonstrate the validity of the model. A nonlinear control law was derived and was shown to behave well even when there were significant modeling and payload inertia uncertainties. The behavior of this control law, however, was shown to deteriorate when accurate measurements were not available. To alleviate this problem, a correction term

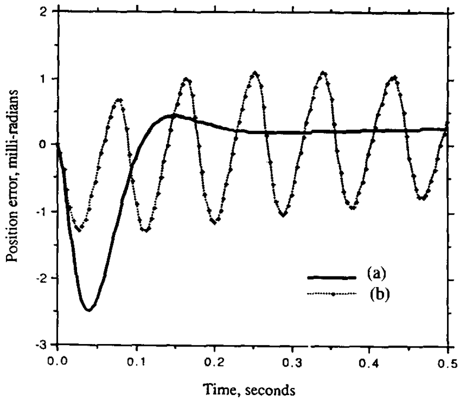

Fig. 10. Time histories of position error for the robust controller with various error bound sizes ϕ: (a) $\pi = 10^{10}$, $\delta q_1 = \delta q_2 = 0.35$, $\Delta f_4 = \Delta f_5 = 10^{-5}$; (b) $\pi = 10^{10}$, $\delta q_1 = \delta q_2 = 0.75$, $\Delta f_4 = \Delta f_5 = 10^{-5}$.

was derived and appended to the nonlinear controller to improve the robustness of the system. It was demonstrated that by appropriately choosing maximum bounds on the uncertainties in the system, favorable results are accomplished. Further investigation through computer simulations indicated that it is possible to create undesirable oscillations in the system if the controller law is not properly defined.

References

[1] H. Asada and K. Youcef-Toumi, *Direct Drive Robots: Theory and Practice*. Cambridge, MA: MIT Press, 1987.

[2] A. E. Fitzgerald, C. Kingsley, and S. D. Umans, *Electric Machinery*. New York: McGraw-Hill, 1983, 4th ed.

[3] S. Gutman, "Uncertain dynamical systems—A lyapunov min-max approach," *IEEE Trans. Automat. Contr.*, vol. AC-24, no. 3, pp. 437-443, June 1979.

[4] I. J. Ha and E. G. Gilbert, "Robust tracking in nonlinear systems," *IEEE Trans. Automat. Contr.*, vol. AC-32, no. 9, pp. 763-771, Sept. 1987.

[5] N. Hemati, "Modeling, analysis, and tracking control of brushless dc motors for robotic applications," Ph.D. thesis, Sibley Sch. Mech. Aerospace Eng., Cornell Univ., 1988.

[6] N. Hemati and M. C. Leu, "A complete model characterization of brushless dc motors," in *Proc. IEEE Ind. Appl. Soc.*, Ann. Mtg. (Seattle, WA), Oct. 1990.

[7] N. Hemati and M. C. Leu, "Nonlinear tracking control of brushless dc motors for high-performance applications," in *Proc. 28th IEEE Conf. Decision Contr.* (Tampa, FL), Dec. 1989, pp. 527-530.

[8] L. R. Hunt, R. Su, and G. Meyer, "Design for multi-input nonlinear systems," in *Differential Geometric Control Theory*. Cambridge, MA: Birkhauser, 1982.

[9] M. Ilic-Spong, R. Marino, S. M. Peresada, and D. G. Taylor, "Feedback linearizing control of switched reluctance motors," *IEEE Trans. Automat. Contr.*, vol. AC-32, no. 5, pp. 371-379, May 1987.

[10] M. Ilic-Spong, T. J. E. Miller, S. R. MacMinn, and J. S. Thorp, "Instantaneous torque control of electric motor devices," *IEEE Trans. Power Electron.*, vol. PE-2, no. 1, pp. 55-61, Jan. 1987.

[11] P. C. Krause, *Analysis of Electric Machinery*. New York: McGraw-Hill, 1986.

[12] G. Leitman, "On the efficacy of nonlinear control in uncertain linear systems," *Dynamic Syst. Meas. Contr.*, vol. 102, pp. 95-102, June 1981.

[13] M. W. Spong, J. S. Thorp, and J. M. Kleinwaks, "The control of robot manipulators with bounded input, Part II: Robustness and disturbance rejection," in *Proc. 23rd IEEE Conf. Decision Contr.* (Las Vegas, NV), Dec. 1984.

[14] M. Vidyasagar, "System theory and robotics," *IEEE Contr. Syst. Mag.*, pp. 16-17, Apr. 1987.

[15] D. C. Youla and J. J. Bongiorno Jr., "A floquet theory of the general rotating machine," *IEEE Trans. Circuits Syst.*, vol. CAS-27, no. 1, pp. 15-19, Jan. 1980.